ASSESSING MANGANESE CONCENTRATIONS IN GROUNDWATER ACROSS THE SHENANDOAH VALLEY, VA

CHRISTOPHER GOLDMANN, Trinity University
Project Advisor: Brady Ziegler

INTRODUCTION

Elevated concentrations of aqueous manganese (Mn^{2+}) in drinking water can have a multitude of adverse human health effects and undesirable aesthetic consequences. Chronic exposure to Mn^{2+} concentrations $\geq$ 100 parts per billion (ppb) can elicit a variety of negative health effects including reduced IQ, increased infant mortality and cancer rates, and increased risk of Parkinson's disease (Bouchard et al., 2011; Langley et al., 2015; Sanders et al., 2014; Spangler and Spangler, 2009; Spangler and Reid, 2010). The Environmental Protection Agency (EPA) has established a lifetime chronic exposure maximum contaminant level (MCL) of 300 ppb (U.S. Environmental Protection Agency, 2004), though negative health effects have been documented with chronic exposure to Mn $\geq$ 100 ppb (Ljung and Vahter, 2007; Langley et al., 2015; Sanders et al., 2014). Additionally, the EPA has set a 1-day and 10-day health advisory (HA) for acute exposure to Mn^{2+} at 1,000 ppb and a secondary maximum contaminant level (SMCL) for Mn^{2+} at 50 ppb to avoid bitter metallic tastes and staining (U.S. Environmental Protection Agency, 2004).

This study investigates Mn^{2+} concentrations in groundwater in the Shenandoah Valley, Virginia, where at least 36% of the population uses private wells for drinking water (Virginia State Water Resources Plan, 2015; U.S. Census Bureau, 2019). While regular testing and treatment of municipal public water supplies is required by U.S. law, monitoring private supplies is optional. Water quality monitoring services are provided by the Virginia Household Water Quality Program (VAHWQP; www.wellwater.bse.vt.edu) upon request.

The Shenandoah Valley falls within the Valley and Ridge Province, bordered by the Blue Ridge Province to the east and the Appalachian Plateaus Province to the west. The Valley and Ridge Province is geologically complex, with generalized host lithologies including shale, black shale, dolostone, limestone, sandstone, igneous, and metamorphic facies (USGS, 2003).

Mn can be introduced to groundwater through a variety of geogenic and anthropogenic mechanisms. Most commonly, high concentrations of dissolved organic carbon (DOC) in aquifer soils and sediments can stimulate microbial populations and rapidly deplete dissolved oxygen to generate a reducing environment, under which Mn(IV)-oxides, ubiquitous in soils and sediments, are reductively dissolved to aqueous Mn^{2+} (Di-Ruggiero and Gounot, 1990). This reaction is shown in Eq. 1, where CH_2O represents generalized organic matter.

$$2MnO_2 + CH_2O + 3H^+ = HCO^{3-} + 2Mn^{2+} + 2H_2O \quad \text{(Eq. 1)}$$

Thus, environments with shallow anoxic water tables, elevated DOC in host soils, and/or host lithologies containing organic matter (e.g., shale) often contain elevated Mn^{2+} (McMahon et al. 2018). Additionally, soil weathering may increase the quantity of Mn(IV)-oxides available for reductive dissolution. For example, in the Piedmont Plateau of North Carolina, chemical weathering of near-surface soil and saprolite dissolves primary Mn(II,III)-bearing minerals that precipitate as secondary Mn(III,IV)-oxides near the water table. Under reducing conditions, these secondary Mn oxides dissolve and mobilize Mn^{2+} in groundwater (Gillispie et al., 2016).

Possible anthropogenic sources of Mn to groundwater

include, but are not limited to, Mn mines, pesticides, and gasoline. Improperly-reclaimed or abandoned historic Mn ore mines exist throughout the Valley, thus serving as a potential source of Mn^{2+} to groundwater if Mn-bearing minerals are mobilized and exposed to reducing conditions (Hue et al. 2001; Li et al. 2007). The application of fungicides with Mn-containing chemicals Maneb® and Mancozeb® in orchards may lead to Mn^{2+} contamination of groundwater via runoff (Semu and Singh, 1995), and the Mn-bearing molecule methylcyclopentadienyl manganese tricarbonyl (MMT) is used as an additive in gasoline and can accumulate along roadways from engine exhaust which may also introduce Mn^{2+} to groundwater via runoff (Lytle et al., 1995).

The objective of this study is to isolate Mn groundwater contamination mechanisms specific to the Shenandoah Valley. By identifying variables associated with elevated Mn and identifying the primary mechanism by which Mn^{2+} enters groundwater, the Valley's population reliant on private drinking wells can better avoid many of the adverse health effects associated with low level chronic exposure to Mn^{2+} via drinking water.

METHODS

Groundwater Collection and Analyses

This study utilizes well water data from VAHWQP and the United States Geological Survey (USGS) National Water Information System (NWIS). The VAHWQP data set contains samples collected at private residences between 2009 and 2019. Samples were collected from the tap inside privately-owned structures under a single address after five minutes of continuous flushing. Samples were analyzed for NO_3^- and F^- using ion chromatography, while inductively coupled mass spectrometry (ICP-MS) was used to measure all other analytes (Na, Mg, Al, Si, P, SO4, K, Ca, V, Cr, Fe, Mn, Co, Ni, Cu, Zn, As, Mo, Ag, Cd, Sn, Pb, Cl, Ti, Se, Sr, Ba, and U). In concert with the testing of private water supplies, property owners answered questionnaires; topics addressed in the questionnaire included (but were not limited to) whether a water treatment system was present, plumbing construction materials, noticeable aesthetic deficiencies of water, proximity of the property to environmental hazards such as landfills, and whether any member of the household had been sick in the past 30 days.

Data from the USGS NWIS were compiled and reported by McMahon et al. (2018). NWIS data was collected between 1988 and 2017; all samples were collected directly from wells rather than household taps and analyzed with ICP-MS. Data from VAHWQP and NWIS were combined into a single data set, resulting in 1587 unique sampling locations and 1906 individual samples. Thus, 319 samples were collected at duplicate locations at different points in time; samples reporting the highest Mn^{2+} concentrations were prioritized if multiple samples existed for a given location.

Geospatial Analyses

The combined water chemistry data set was imported into ArcGIS Pro 2.8.3 for geospatial analysis. Publically-available geospatial data used in this study include: a shapefile of surface water (streams/rivers) (Virginia Department of Environmental Quality), geologic structures including faults, dikes, and sills (Dicken et al., 2005), generalized lithology (Dicken et al., 2005), historic Mn mine locations (Bureau of Land Management, compiled by www.thediggings.com), orchard proximity (from VAHWQP questionnaire), and roadways (U.S. Census Bureau, Department of Commerce). These data were plotted with the combined VAHWQP/NWIS data set to elucidate potential geospatial controls on elevated Mn concentrations.

Statistical analyses

Multivariate statistical analyses can be useful for large chemical databases to elucidate patterns that inform geochemical mechanisms and processes occurring in a given system. Therefore, the combined VAHWQP/NWIS data set was passed through a principal component analysis (PCA) in an attempt to identify processes impacting groundwater chemistry in the Shenandoah Valley. PCA is a dimension reduction method of multivariate data that aims to identify trends and variation in the data by reducing it to dimensionless latent variables (principal

components) that account for the maximum variance in the multivariate data set. The amount of variance in the data set that is explained decreases with each additional principal component.

PCA output is generally presented as a two-dimensional biplot that compares principal component one (PC1, x-axis) vs principal component two (PC2, y-axis), which explain the most and second-most variance in the data, respectively. Points, known as scores, plot the values of PC1 and PC2 for each sample. Vectors move away from the origin (which represents the geometric mean). The length of a variable's vector indicates the amount of control that variable exerts on the principal component in the vector's direction. Vectors that point in the same direction along a principal component axis are closely related, whereas vectors that point in the opposite direction along a principal component axis are inversely related, but still controlled by that same principal component. For example, if a principal component reflects redox state, one could expect dissolved Fe and Mn vectors to point in the same direction along the principal component axis and point in the opposite direction of dissolved oxygen.

RESULTS

The spatial distribution of Mn^{2+} concentrations in groundwater is depicted in Fig. 1. The majority of elevated Mn^{2+} samples (>100 ppb) are located in the northern part of the Valley and towards the Valley center. Elevated Mn samples occur in curvilinear clusters, and isolated high Mn^{2+} samples surrounded by low Mn^{2+} (<100 ppb) rarely occur. Conversely, groundwater samples near the Valley's southern end and along the eastern and western margins are comparatively low in Mn^{2+}.

Anthropogenic Mn Sources

Fig. 2A displays groundwater Mn^{2+} concentrations with potential anthropogenic Mn inputs such as roads, orchards, and historic Mn mines. Interstate 81 runs the length of the valley from north to south; while there is elevated Mn^{2+} near roadways in the north, this trend is absent in the south. Historic Mn mines are concentrated along ridges near the southeastern margin of the Valley; a cluster of mines also occurs
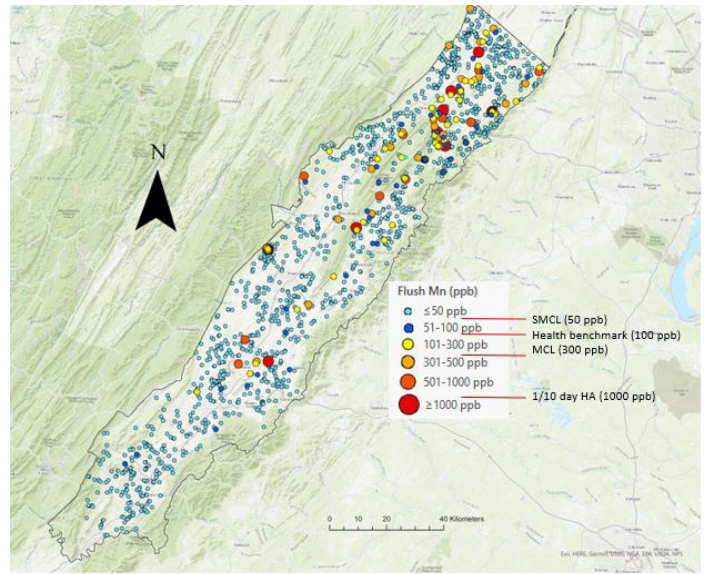

Figure 1. Spatial distribution of groundwater Mn^{2+} concentrations in the Shenandoah Valley.

on the northwestern margin of Massanutten Mountain Range toward the Valley's northern end. While these historic mines reflect the presence of Mn ores, their existence does not seem to influence groundwater Mn^{2+} concentrations in the vicinity. Orchards are sparsely distributed near the Valley's western margin. Given the lack of orchards in proximity to samples with elevated Mn^{2+}, their existence does not seem to influence groundwater Mn^{2+} concentrations in the region.

Geogenic Mn Sources

Fig. 2B displays groundwater Mn^{2+} concentrations along with surface water (streams/rivers) in the Valley.
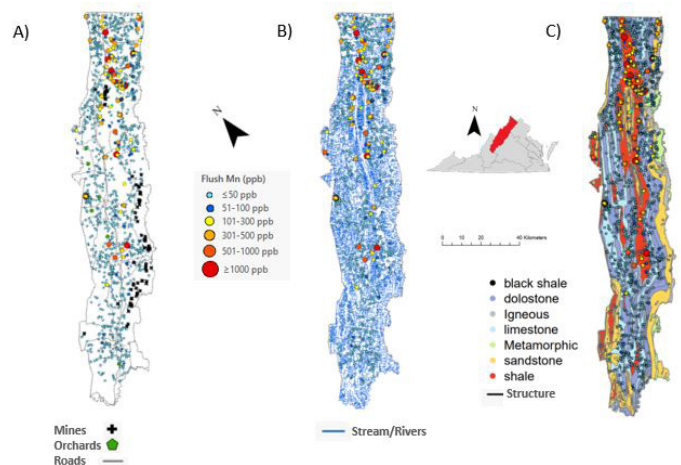

Figure 2. Map of groundwater sample Mn concentrations (ppb) with A) anthropogenic features; B) surface waters; and C) host lithology and geologic structure (faults, dikes, and sills).
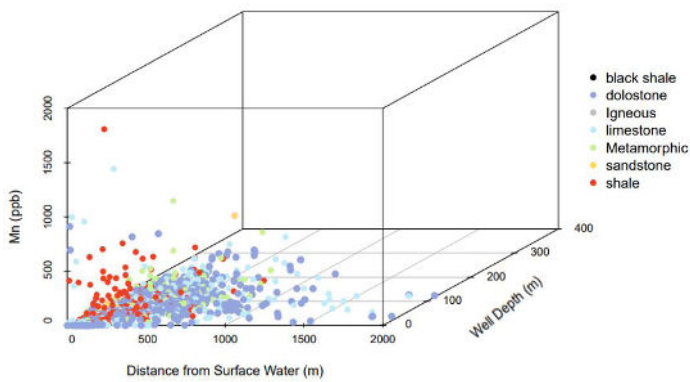
3

Figure 3. 3D scatterplot of sample Mn concentrations (ppb), distance to surface water (m), and well depth (m): all samples are categorized by host lithology.

Generally, groundwater samples with elevated Mn^{2+} concentrations (>100 ppb) tend to occur in closer proximity to surface water, and Mn^{2+} concentrations decrease with distance. To quantitatively support this observation, the shortest linear distance between sample locations and surface water was calculated and compared in conjunction with well depth and Mn^{2+} concentration (Fig. 3). Due to the dense distribution of surface waters in the valley, the vast majority of samples are within 1000 m of surface water. While the average distance of elevated Mn^{2+} samples from surface water was 206 m, the average distance of all low Mn^{2+} samples (<100 ppb) is notably farther at 304 m. In particular, elevated Mn^{2+} in groundwater often occurs near the headwaters of tributary streams/rivers.

Aquifer lithology carries important implications for groundwater Mn^{2+} concentrations (Fig. 2C). Due to a high average thickness of lithologic units in the region, it is assumed that surface lithology is indicative of aquifer lithology (Trapp, Jr. and Horn, 1997). As is consistent with the findings of McMahon et al. (2018), siliciclastic sedimentary lithologies (shales and sandstones) have the highest average groundwater Mn^{2+} concentrations. A majority of elevated Mn^{2+} samples in the Valley occur in the Martinsburg Formation, which is predominantly shale and underlies the majority of elevated Mn^{2+} samples in the northern part of the Valley as well as a few samples toward the southern extent where it outcrops. However, a few elevated Mn^{2+} samples occur in carbonate lithologies throughout the Valley. This typically occurs near a boundary between carbonate and shale lithologies, thus shales are still in close proximity to these samples.

The percentage of samples in exceedance of aesthetic and health benchmarks (Table 1) help inform lithologic controls on groundwater Mn concentrations in the valley. Only 10 samples exceeded the EPA 1 and 10-day health advisory limit of 1000 ppb, 60 samples exceeded the lifetime chronic exposure MCL of 300 ppb, 111 samples exceeded the 100 ppb potential health benchmark, and 148 samples exceeded the SMCL of 50 ppb. Relative to other lithologies, a higher percentage of samples collected in shale and sandstone lithologies exceeded MCL, SMCL, and HA thresholds. For example, approximately 25% of all samples taken in sandstone and shale exceeded the 50 ppb SMCL, while only 8% of all samples (regardless of lithology) exceeded 50 ppb.

Statistical Analysis

A PCA biplot identifies two principal components that explain the maximum variance among all geochemical analytes in the combined VAHWQP/NWIS data set (Fig. 4). PC1 explains 32.64% of the total variance in the data set, and is heavily influenced by Ca, Mg, and hardness in an elongated, tight cluster of vectors in the direction of positive PC1 space. Other divalent trace metals such as Sr^{2+} and Ba^{2+} exert an influence on PC1 in the positive direction, ultimately plotting with the Ca, Mg, and hardness cluster. This clustering can be explained by the tendency of Sr^{2+} and Ba^{2+} to substitute freely for Ca^{2+} and Mg^{2+} in the carbonate matrix. In contrast, the Na vector points in the opposite direction, into negative PC1 space. No other analytes associate strongly with Na in PC1 space. Interestingly, a substantial number of samples from limestone and dolostone aquifers associate with Na and not Ca or Mg, as would be expected based on matrix mineralogy.

Principal component 2 (PC2) explains 13.08% of the total variance. Nitrate (shown as NO3_N) exerts control on PC2 in the positive dimension and is

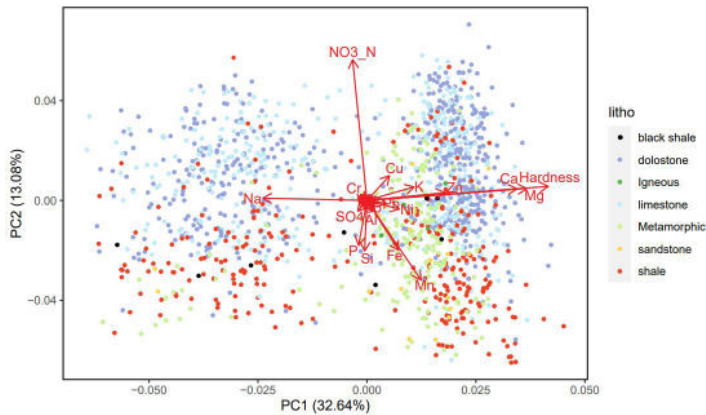| Table 1: % of wells in exceedance of:				
Lithology	50 ppb	100 ppb	300 ppb	1000 ppb
Black shale (n = 8)	0	0	0	0
Dolostone (n = 757)	2	0.9	1	0
Igneous (n = 4)	0	0	0	0
Limestone (n = 584)	3	2	2	1
Metamorphic (n = 210)	13	10	6	0
Sandstone (n = 16)	25	13	6	0
Shale (n = 326)	26	21	10	2
Overall (n = 1906)	8	6	3	0.5

Figure 4. Results of a principal component analysis (PCA) biplot of 25 analytes from the combined VAHWQP and NWIS data set. The following analytes were removed due to incomplete data: Cl, Ti, Se, Sr, Ba, and U.

juxtaposed with Mn and Fe, which are tightly coupled and exert the most control in the negative PC2 dimension. Additionally, Si and P exert control in the negative PC2 dimension, though to a lesser extent than Mn and Fe. Separation by lithology is more prevalent in PC2 than in PC1: while carbonates occur in both positive and negative PC2 space, they are clustered toward the positive and weakly negative PC2 space. In contrast, shales are far more abundant in negative PC2 space.

DISCUSSION

From the PCA, and in conjunction with the VAHWQP questionnaire, it can be inferred that PC1 is reflective of in-home water treatment, including but not limited to water softener systems that remove Ca and Mg in exchange for Na from water softening salts. Thus, untreated samples fall in positive PC1 space and most accurately reflect the groundwater chemistry, whereas treated samples fall in negative PC1 space. A clear separation of samples by host lithology does not occur along the PC1 axis, as might be expected if PC1 is controlled by treatment and is independent of processes occurring in host lithologies. While metamorphic samples tend to fall disproportionately in positive PC1 space, all other lithologies are equally distributed across the PC1 axis. This reinforces the notion that PC1 is water treatment status: whether or not a sample has undergone treatment is completely independent of host lithology.

Given the dichotomy between NO_3^- and aqueous Mn

and Fe, PC2 likely evinces redox conditions: positive PC2 space reflects oxidizing conditions while negative PC2 space reflects reducing conditions. This is further supported by host lithology: abundant organic matter within shales typically evokes reducing conditions through decay processes, and the majority of shale samples plot in negative PC2 space. Conversely, the majority of carbonate samples plot in positive PC2 space, thus indicating that weathered carbonates in this karst terrain are more oxic relative to shales.

Most trace metals do not heavily influence either PC1 or PC2, as indicated by relatively short vectors. However, they trend toward positive PC1 space and negative PC2 space, which is indicative of untreated samples under reducing conditions.

CONCLUSIONS

This study has determined that a combination of redox conditions and host lithology is the primary mechanism contributing to elevated Mn^{2+} concentrations in groundwater in select areas within the Shenandoah Valley. Elevated Mn^{2+} samples are located primarily in shale host lithologies, which are associated with reducing conditions that reductively dissolve Mn oxides to mobilize Mn^{2+} to groundwater in the vicinity. Conversely, and as is consistent with the findings of McMahon et al. (2018), weathered carbonates in karst terrains are associated with an oxic environment that stabilizes Mn in the solid phase and reduces the quantity of Mn^{2+} available in groundwater. Overall, those who source drinking water from wells in the Shenandoah Valley should be cautious of consuming untreated water within shale lithologies, whereas water sourced from carbonate lithologies is relatively safe. Future work will involve the isolation of only untreated samples within the VAHWQP data set for further analysis.

ACKNOWLEDGEMENTS

REFERENCES

Bjørklund, G., Chartrand, M.S., and Aaseth, J., 2017, Manganese exposure and neurotoxic effects in children: Environmental Research, v. 155, p. 380–384, doi:10.1016/j.envres.2017.03.003.

Bouchard, M., Laforest, F., Vandelac, L., Bellinger, D., and Mergler, D., 2007, Hair Manganese and Hyperactive Behaviors: Pilot Study of School-Age Children Exposed through Tap Water: Environmental Health Perspectives, v. 115, p. 122–127, doi:10.1289/ehp.9504.

Bouchard, M.F., Sauvé, S., Barbeau, B., Legrand, M., Brodeur, M.-È., Bouffard, T., Limoges, E., Bellinger, D.C., and Mergler, D., 2011, Intellectual Impairment in School-Age Children Exposed to Manganese from Drinking Water: Environmental Health Perspectives, v. 119, p. 138–143, doi:10.1289/ehp.1002321.

Dicken, Connie L., Nicholson, Suzanne W., Horton, John D., Kinney, Scott A., Gunther, Gregory, Foose, Michael P., and Mueller, Julia A.L., 2005, Integrated Geologic Map Databases for the United States: Delaware, Maryland, New York, Pennsylvania, and Virginia: U.S. Geological Survey Open-File Report 2005-1325, U.S. Geological Survey, Reston, VA.

Di-Ruggiero, J., and A. M. Gounot. "Microbial manganese reduction mediated by bacterial strains isolated from aquifer sediments." Microbial ecology 20.1 (1990): 53-63.

Force, E. R., & Cox, L. J, 1991. Manganese contents of some sedimentary rocks of Paleozoic Age in Virginia. U.S. Geological Survey Bulletin 1916.

Gillispie, E.C., Austin, R.E., Rivera, N.A., Bolich, R., Duckworth, O.W., Bradley, P., Amoozegar, A., Hesterberg, D., and Polizzotto, M.L., 2016, Soil Weathering as an Engine for Manganese Contamination of Well Water: Environmental Science & Technology, v. 50, p. 9963–9971, doi:10.1021/acs.est.6b01686.

Hafeman, D., Factor-Litvak, P., Cheng, Z., van Geen, A., and Ahsan, H., 2007, Association between Manganese Exposure through Drinking Water and Infant Mortality in Bangladesh: Environmental Health Perspectives, v. 115, p. 1107–1112, doi:10.1289/ehp.10051.

Hue, N. V.; Vega, S.; Silva, J. A. Manganese Toxicity in a Hawaiian Oxisol Affected by Soil PH and Organic Amendments. Soil Science Society of America Journal 2001, 65 (1), 153–160. https://doi.org/10.2136/sssaj2001.651153x.

Hue, N.V., Vega, S., Silva, J.A., 2001. Manganese Toxicity in a Hawaiian Oxisol Affected by Soil pH and Organic Amendments. Soil Sci. Soc. Am. J. 65, 153–160. https://doi.org/10.2136/sssaj2001.651153x

Khan, K. et al., 2012, Manganese exposure from drinking water and children's academic achievement: NeuroToxicology, v. 33, p. 91–97, doi:10.1016/j.neuro.2011.12.002.

Langley, R., Kao, Y., Mort, S., Bateman, A., Simpson, B., and Reich, B., 2015, Adverse neurodevelopmental effects and hearing loss in children associated with manganese in well water, North Carolina, USA: Journal of Environmental and Occupational Science, v. 4, p. 62, doi:10.5455/jeos.20150403060427.

Li, M.S., Luo, Y.P., Su, Z.Y., 2007. Heavy metal concentrations in soils and plant accumulation in a restored manganese mineland in Guangxi, South China. Environmental Pollution 147, 168–175. https://doi.org/10.1016/j.envpol.2006.08.006.

Ljung, K., and Vahter, M., 2007, Time to Re-evaluate the Guideline Value for Manganese in Drinking Water? Environmental Health Perspectives, v. 115, p. 1533–1538, doi:10.1289/ehp.10316.

Lytle, C. M.; Smith, B. N.; McKinnon, C. Z. Manganese Accumulation along Utah Roadways: A Possible Indication of Motor Vehicle Exhaust Pollution. Science of The Total Environment 1995, 162 (2), 105–109. https://doi.org/10.1016/0048-9697(95)04438-7.

McMahon, P.B., Belitz, K., Reddy, J.E., and

Johnson, T.D., 2018, Elevated Manganese Concentrations in United States Groundwater, Role of Land Surface–Soil–Aquifer Connections: Environmental Science & Technology, v. 53, p. 29–38.

Sanders, A.P., Desrosiers, T.A., Warren, J.L., Herring, A.H., Enright, D., Olshan, A.F., Meyer, R.E., and Fry, R.C., 2014, Association between arsenic, cadmium, manganese, and lead levels in private wells and birth defects prevalence in North Carolina: a semi-ecologic study: BMC Public Health, v. 14, p. 955, doi:10.1186/1471-2458-14-955.

Semu, E., Singh, B.R., 1995. Accumulation of heavy metals in soils and plants after long-term use of fertilizers and fungicides in Tanzania. Fertilizer research 44, 241–248. https://doi.org/10.1007/BF00750931.

Spangler, A.H., and Spangler, J.G., 2009, Groundwater Manganese and Infant Mortality Rate by County in North Carolina: An Ecological Analysis: EcoHealth, v. 6, p. 596–600, doi:10.1007/s10393-010-0291-4.

Spangler, J.G., and Reid, J.C., 2010, Environmental Manganese and Cancer Mortality Rates by County in North Carolina: An Ecological Study: Biological Trace Element Research, v. 133, p. 128–135, doi:10.1007/s12011-009-8415-9.

Trapp, Jr., H. and Horn, M.A., 1997, U.S. Geological Survey Ground Water Atlas of the United States: Delaware, Maryland, New Jersey, North Carolina, Pennsylvania, Virginia, West Virginia. HA 730-L

U.S. Census Bureau, Department of Commerce: TIGER/Line Shapefile, 2015, state, Virginia, Primary and Secondary Roads State-based Shapefile

U.S. Census Bureau, 2019, Population of Virginia by County.

U.S. Environmental Protection Agency, 2004, Drinking Water Health Advisory for Manganese.

U.S. Geological Society, 2003. Virginia geologic map data.

Virginia Department of Environmental Quality, Office of Ecology, Water Monitoring & Assessment Program

Virginia State Water Resources Plan, 2015.

Yager, R.M., Voss, C.I., and Southworth, S., 2009, Comparison of alternative representations of hydraulic-conductivity anisotropy in folded fractured-sedimentary rock: modeling groundwater flow in the Shenandoah Valley (USA): Hydrogeology Journal, v. 17, p. 1111–1131, doi:10.1007/s10040-008-0431-x.